

Pulse based sensor networking using mechanical waves through metal substrates

S. Lorenz, B. Dong, Q. Huo, W.J. Tomlinson Jr. and S. Biswas

Michigan State University, Department of Electrical- and Computer Engineering, 2120 Engineering Building, East Lansing, MI, USA 48824

ABSTRACT

This paper presents a novel wireless sensor networking technique using ultrasonic signal as the carrier wave for binary data exchange. Using the properties of lamb wave propagation through metal substrates, the proposed network structure can be used for runtime transport of structural fault information to ultrasound access points. Primary applications of the proposed sensor networking technique will include conveying fault information on an aircraft wing or on a bridge to an ultrasonic access point using ultrasonic wave through the structure itself (i.e. wing or bridge). Once a fault event has been detected, a mechanical pulse is forwarded to the access node using shortest path multi-hop ultrasonic pulse routing. The advantages of mechanical waves over traditional radio transmission using pulses are the following: First, unlike radio frequency, surface acoustic waves are not detectable outside the medium, which increases the inherent security for sensitive environments in respect to tapping. Second, event detection can be represented by the injection of a single mechanical pulse at a specific temporal position, whereas radio messages usually take several bits. The contributions of this paper are: 1) Development of a transceiver for transmitting/receiving ultrasound pulses with a pulse loss rate below $2 \cdot 10^{-5}$ and false positive rate with an upper bound of $2 \cdot 10^{-4}$. 2) A novel one-hop distance estimation based on the properties of lamb wave propagation with an accuracy of above 80%. 3) Implementation of a wireless sensor network using mechanical wave propagation for event detection on a 2024 aluminum alloy commonly used for aircraft skin construction.

Keywords: Wireless Sensor Networks, Ultrasound, Packet less Communication, Event Monitoring, Transceiver Design, Energy Efficient Networks

1. INTRODUCTION

This paper introduces an energy efficient paradigm for event detection and localization in wireless sensor networks (WSN). Contrary to packet based data exchange, the method described in this paper uses pulse switching. By using a narrow pulse, binary information is exchanged between nodes. The primary application for this protocol is found in event detection and localization, where a binary alphabet for data exchange is sufficient. Traditional event detection sensor networks use multi bit packets in order to exchange data with each other. By only using a single pulse, the overhead per data exchange can be reduced heavily, compared to the radio based approaches. One example application for pulsed based event monitoring is found in determining the structural health of bridges. Another application is found in monitoring aircraft wings for structural failure. Since most objects to be monitored are rather large in dimension, multiple nodes are necessary in order to detect a change in the structural health at any given point on the medium itself. This leads to the conclusion that multi-hop network architecture is indispensable. Hence, a specialized MAC routing frame¹ has been developed. Using this frame structure, the origin of a pulse is maintained in a multi-hop network. Therefore, the pulse-switching network is of interest for large structures.

Ultrasonic waves are being used to abstract a single pulse for data exchange between two nodes. Since the used waves are of low power, the structure is not being affected in respect to its health. In order to be able to use the proposed frame structure¹, the properties of ultrasonic wave propagation on a certain medium have to be considered for the size of a slot. In order to have a realistic test environment, the system is being tested on a 2024 aluminum plate. The structure is 3.6m long, 1.2m wide and 1mm thick. Hence, the dimension of this medium is rather close to an F-16 aircraft wing.

The contributions in this paper are the following: First, an ultrasonic pulse transceiver for ultrasonic pulse switching in packet-less wireless sensor networks has been developed. Second, a reliable pulse based communication link on a solid substrate has been established. Third, a novel distance estimation algorithm for in-structure communication has been developed. Finally, a frame structure for multi hop communication has been implemented.

Huo¹ et al. already designed a pulsed based communication model for WSN. In their publication about cellular pulse switching architectures for binary event sensing, they described a network protocol that uses pulsed communication in the ultra wideband (UWB) domain. Their approach of designing a frame structure in order to enable nodes for multi hop communication has been used as a reference for designing the frame structure in this publication. In this paper, ultrasonic pulses have been chosen over a UWB pulses. Tomlinson² et al. investigated the propagation of ultrasound in metal substrates. Their research focused on the general behavior of ultrasonic wave propagating through metal substrates, and especially and aircraft wing. However, in their work they do not have an embedded version of their system to be used in a WSN. Saulnier³ et al. present a through wall communication mechanism, using ultrasonic pulses. However, they also do not mention having an embedded version to be used in a WSN. X. Zhao⁴ et al. presented an ultrasonic crack detection mechanism for metallic structures. Their work can also be used to monitor the growth of a faulty entity of a structure. Their type of technology uses 100V input signals at 350kHz, which is impractical and inefficient for a WSN, powered by batteries. Giurgiutiu^{5,6} et al present a solution to detect a faulty in aging aircraft wings, using piezoelectric wafer active sensor (PWAS). In their work they presented a mechanism to introduce ultrasonic pulses at 300kHz for crack detection. Their work is related to the work that has been done in this publication. However, we propose a hardware design for pulse communication, while Giurgiutiu^{5,6} et al. focus their work on crack detection.

2. SYSTEM ARCHITECTURE

2.1 Hardware design

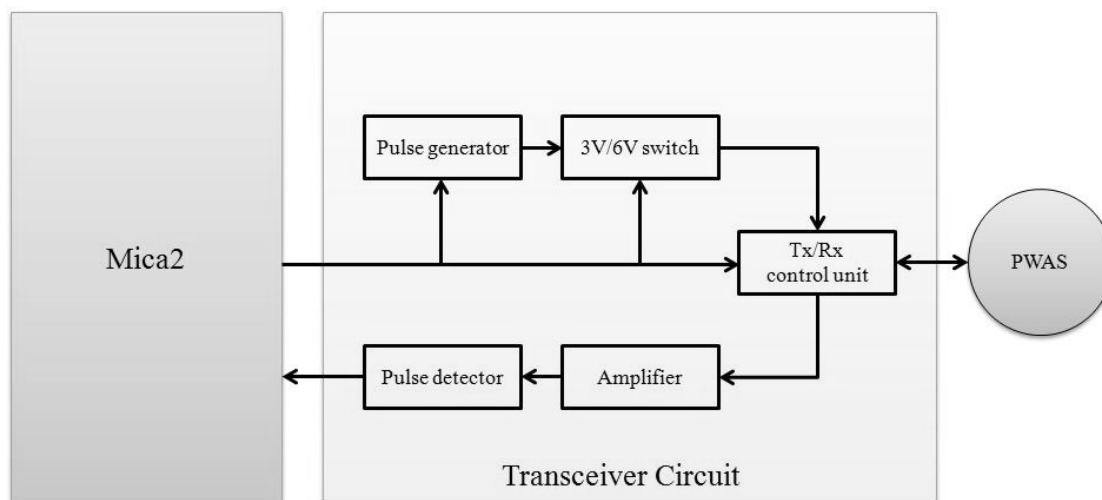


Figure 1. Block diagram of the ultrasonic pulse switching hardware platform

In order to exchange binary information in a WSN using ultrasonic pulses, an ultrasonic transceiver is designed and implemented, which is connected to a widely used sensor platform (Mica2). The transceiver injects ultrasonic pulses using a PWAS from APC International (D-9.55mm-1.00mm-850 WFB). In order to determine the resonance frequency of the PWAS, the received signal strength has been measured over a range of frequencies, while keeping the input voltage constant. One PWAS injected a continuous (sinusoidal) signal, while a second PWAS of same type was used to measure the received signal strength. In figure 2, the results from this experiment are being illustrated. Since the PWAS was most sensitive at roughly 245kHz, this frequency has been used to design the system. The transmitter is capable to either inject a 3V or 6V pulse into the medium. Therefore, four AA batteries can power the entire system. 3V pulses are used to deliver information to another node that is one hop away. In this context, one hop is equivalent to a distance of 1 meter. In case of a necessary pulse transmission over a distance greater than a meter, the node chooses to inject a pulse with amplitude of 6V. With the given medium (length: 3.6m, width: 1.2m, thickness: 1mm), a 6V pulse can be detected by a receiver at one corner even if the transmitter is at the farthest corner. The proposed system has the abilities of switching between 3V and 6V transmission modes as well as transition between transmission and reception modes. In

our system, a single PWAS is being used as the transmitter as well as the receiver. Once a node injected a pulse into the medium, the mechanical waves propagate through the structure.

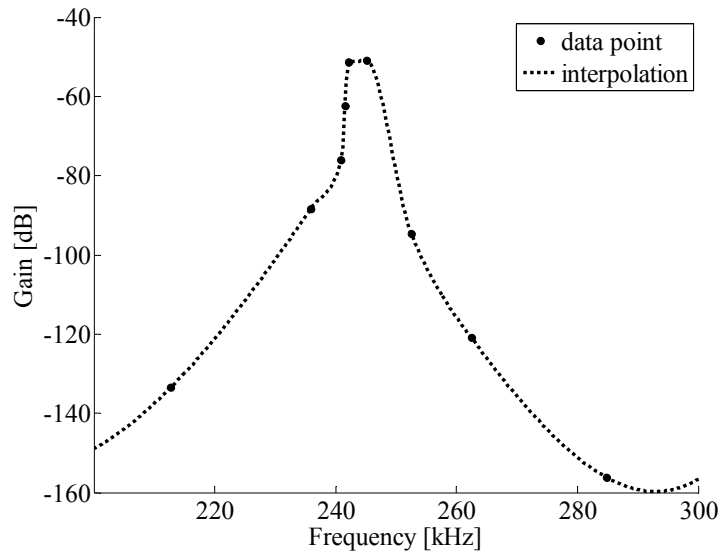


Figure 2. Illustration of the frequency response of the used PWAS (D-9.55mm-1.00mm-850 WFB, APC International)

The propagation of mechanical waves in thin metallic substrates is described by Lamb Waves^{6,7,8}. Lamb waves propagate in two different forms: symmetric (longitudinal waves) and asymmetric (transverse waves). The symmetric waves propagate faster and show lower dispersion. The asynchronous waves, however, propagate slower and have more dispersion. The different symmetric (S) and asymmetric (A) modes are called S_0, S_1, \dots, S_N or A_0, A_1, \dots, A_N . The number of possible modes depends on the thickness of the medium as well as the signal's frequency^{6,7,8}. In 2024 aluminum, the theoretical velocity of the symmetric wave is roughly 5400m/s, while the asymmetric wave propagates with 3100m/s. In the system described in this paper, a 1mm thick 2024 aluminum alloy has been used, and the signals' frequency is set to 245kHz. Therefore, only two waves (S_0 and A_0) can propagate^{6,7,8}.

Another area of interest is the pulse width for a transmission. In order to have a rather efficient way of communication, the optimal pulse width has to be determined for binary pulse switching in solid substrates. If the pulse width is too small, the communication range may be insufficient so that more nodes are needed to cover an object of interest. If the pulse width is chosen to large, energy is being wasted. Therefore, an experiment to determine the ideal pulse width will be conducted in the following way: The pulse width at the transmitter will be varied, while the received signal strength at the receiver will be monitored with an oscilloscope. For this experiment, the distance between the transmitter and receiver will be kept constant at 1m.

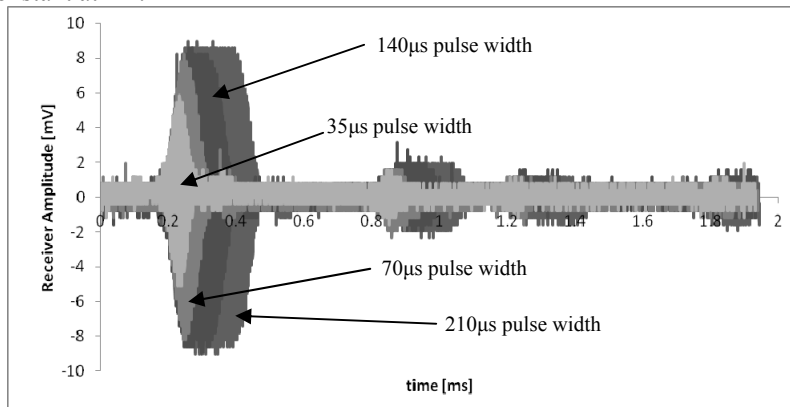


Figure 3. Illustration of received signal strength with a different transmitter pulse widths

In figure 3, the behavior of the receiver is introduced. In this experiment, the focus has been placed on the asymmetric (A_0) wave. This is based on the fact that this type of wave has shown to have a higher peak-to-peak value and therefore was easier to monitor. From the figure above it can be noted that the received signal does not increase in its amplitude after the transmitter pulse width is larger than $70\mu\text{s}$. This is explained by the fact that the receiver PWAS is maximally excited with a transmitting pulse width of $70\mu\text{s}$. Larger values of the pulse width do not result in larger signal amplitude at the receiver, since maximum excitation has already been achieved. Therefore, the pulse width for the system described in this paper has been chosen to be roughly $70\mu\text{s}$.

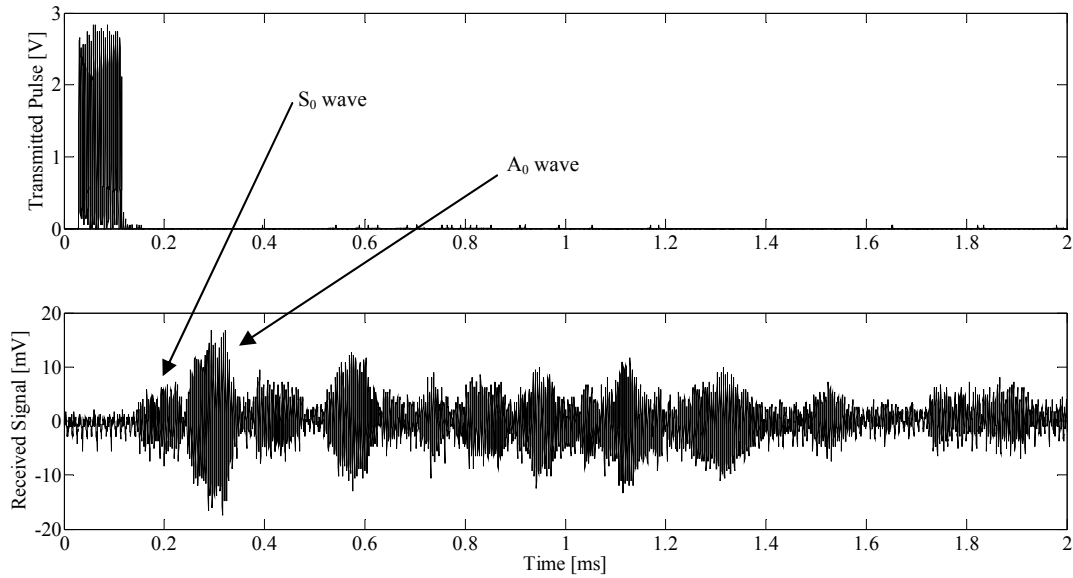


Figure 4. Transmitted and received signals at a distance of 1 meter

In figure 4, an example of transmitted and received signals at a distance of 1 meter is introduced. The received signal shows multiple wave packets. The first wave cluster in the received signal stream is the symmetric wave S_0 , while the second wave packet represents the asymmetric wave A_0 . The figure also shows the echoes of the symmetric and asymmetric wave, coming from the edges of the used structure. In order to properly detect the waves in the medium, the received signal is fed into the receiving signal processing unit, where the signal is amplified and filtered. The output of the receiving module is sent to the Mica2 indicating the start and end of S_0 and A_0 .

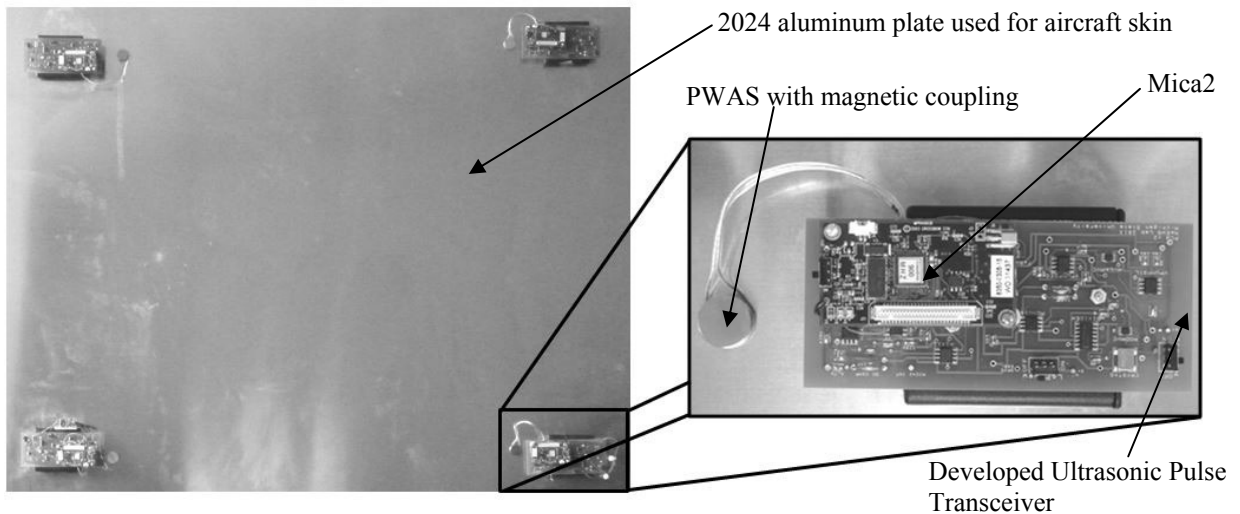


Figure 5. Illustration of multiple nodes mounted on the structure along with a detailed image of one hardware platform

Figure 5 introduces the general setup for a sensor network on the 2024 aluminum plate. In the experimental setup, the nodes are mounted via velcro onto the structure. In this setup, the distance between two nodes is equal to 60cm. On the right side of figure 5, the hardware platform is being presented. The PWAS is glued to a magnet in order to ensure rather consistent, yet temporal and therefore flexible coupling. Another magnet on the back of the aluminum alloy ensures a strong connection onto the structure. The widely used Mica2 node is placed onto the PCB design responsible to work with the pulsed communication described above. This PCB board, however, is mounted to the battery box holding 4AA batteries in order to supply the necessary voltage.

2.2 Algorithms for distance detection

The separation between the received S_0 and A_0 is positively related to the distance between the transmitter and the receiver. This is based on the fact that the symmetric wave has a higher velocity than the asymmetric one. In the following, let the velocity of the symmetric wave be defined as v_s , while the speed of propagation of the asymmetric wave is defined as v_A . Due to the property of lamb waves that the symmetric waves travel faster than asymmetric waves, the receiver may be able to observe isolated S_0 and A_0 . Let time t_s represent the time when S_0 arrives at the receiver and t_a indicates the time of arrival of A_0 . Thus, the time difference can be defined as $\Delta t = t_A - t_S$. Moreover, the distance between the transmitter and receiver may be defined as d . Hence, one can define the time difference between the arrivals of the S_0 and A_0 as:

$$\Delta t = \frac{d}{v_A} - \frac{d}{v_S} \tag{1}$$

From the equation above, it can be seen that the distance can be determined by the following mathematical expression:

$$d = \frac{\Delta t}{v_A^{-1} - v_S^{-1}} \tag{2}$$

Since the velocities of the symmetric and asymmetric waves are known for a given medium, the proposed platform can determine the distance between a transmitter and receiver simply by detecting the difference in arrival of the S_0 and A_0 waves. It has to be mentioned that this algorithm only works for a sufficiently large distance between the transmitter and receiver. For very small distances, there is no visible separation between the symmetric and asymmetric wave. Therefore, the algorithm would not work then. In order to avoid this issue, the minimum size of a cell has been chosen large enough in order to avoid this issue. Knowing the distance between two nodes is important in order to estimate the propagation delay between these two nodes. This parameter will play a key role in future developments for an optimization in respect to node synchronization on the structure.

2.3 Frame structure for multi-hop communication

In this part, a MAC-Routing¹ layer protocol is introduced for multi-hop data exchange using the system introduced in Section 2.1. In the following, one may consider a large structure of interest to be monitored in respect to structural health. Additionally, one may imagine that a single node in the network monitors a certain area of the object. That limited area may be referred as a cell. Therefore, one node in the WSN is responsible to monitor one cell. One requirement for reliable structural health monitoring (SHM) is that every cell has a unique identifier (ID).

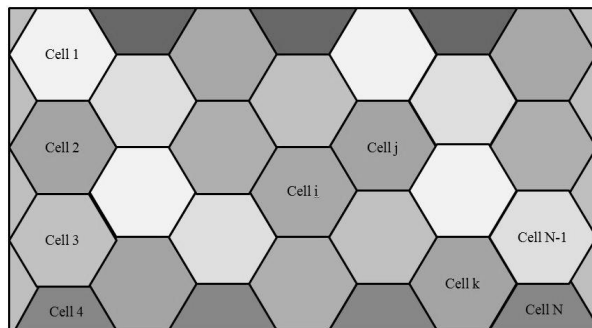


Figure 6. Illustration of a cell-based communication with N nodes on a structure of interest

This unique identifier is necessary in order to localize a faulty section. Figure 6 shows an example of the proposed cellular network. One may consider that nodes from adjacent cells are capable of direct communication, while nodes from non-neighboring cells have to perform multi hop communication in order to exchange information with each other. Moreover, one may consider that each cell only holds a single node. In order to ensure an organized communication, a certain frame structure is necessary. At the beginning of each frame, the sink node injects a 6V synchronization pulse. Applying this at the beginning of each frame allows all nodes in the network to adjust their clocks. The width of this synchronization pulse is denoted with α . The next item in the frame is a dummy slot. This placeholder is needed in order to ignore the delay spread from the synchronization pulse at each node. The size of that dummy slot is identical to the one of a regular slot for data exchange between nodes and equal to λ . The number of regular slots depends on the number of nodes in the network. In order to allow multi-hop communication for event monitoring, the information about the origin has to be maintained. Therefore, a certain structure inside the frame is needed in order to allow multi-hop communication without loss in information about the source.

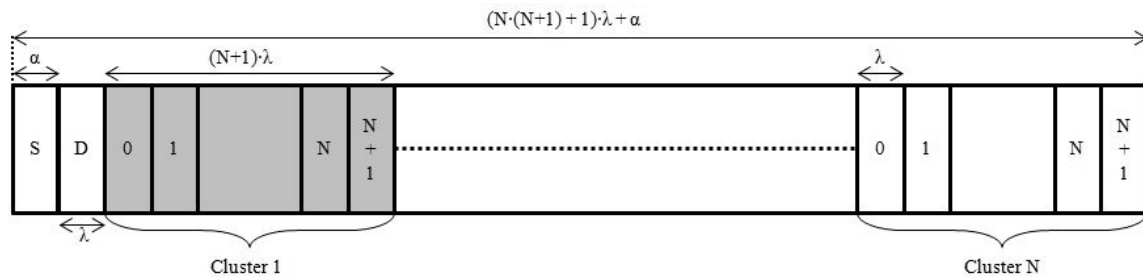


Figure 7. Introduction of the frame structure for N nodes in a WSN using mechanical wave propagation through solid substrates

As seen in figure 7, a frame has the previously mentioned synchronization slot (S), followed by the dummy slot (D). After that, the frame contains N clusters, one for each node in the network. Inside such a cluster, there are $(N+1)$ slots. The first slot of each cluster is used for a communication with the sink, while all other slots are being used to address a pulse to a node on the structure. Therefore, the size of a frame is equal to $(N \cdot (N + 1) + 1) \cdot \lambda + \alpha$.

Once node i ($0 < i < N$) detects an event it will report that observation with an injection of a pulse. Node i will place the pulse in slot 0 of the i^{th} cluster if it is in direct communication range with the sink. Otherwise, node i will place the pulse in the j^{th} slot of the i^{th} cluster, assuming that node j is a neighboring node one hop closer to the sink. Node j , on the other hand, will forward the pulse coming from node i in the i^{th} cluster in the k^{th} slot. Here, it has been assumed that node k is another hop closer to the sink. Node k injects a pulse within the i^{th} cluster in order to maintain the information of the origin. This procedure continues until a node forwards the pulse in slot 0 of the i^{th} cluster, meaning the pulse originated from node i has reached the sink node (ID 0). Applying this mechanism, it is ensured that the sink can determine where the event has been detected even if multiple nodes have forwarded the pulse.

3. EXPERIMENTS

First, the reliability of the communication link between the transmitter and receiver has to be determined. For this, one node is set as a transmitter while a second node has the role of the receiver. The system is monitored at the receiver by a serial port connection to a computer. In order to determine the performance of the link, the pulse loss rate (PLR) as well as the false positive rate (FPR) have to be determined. A coaxial wire connects the transmitting mode with the receiving one. Every ψ ms, the transmitting node starts a new cycle. In every cycle, the transmitter injects a pulse over the coaxial wire while it only injects a pulse every other cycle into the structure. Therefore, the receiver can determine a pulse loss as well as a false positive detection. The PLR and FPR are being determined for various distances as well as different absolute positions on the structure.

Second, the effect of multipath will be determined as well. This parameter is a key factor for the minimum slot size in the frame structure. In order to evaluate this parameter, the transmitter/receiver pair will be placed on the plate on different absolute positions and distances to each other. With the help of an oscilloscope, the delay spread will be determined.

4. RESULTS

4.1 Pulse loss rate and false positive detection

In the following, the PLR and FPR for different distances between the transmitter and receiver are being studied according to the description in section 3. The PLR and FPR have been determined for 0.5m, 0.75m and 1.0m. For distances smaller than 0.5m, the system was not able to distinguish between the S_0 and A_0 wave. Hence, the algorithm to estimate the distance between the two nodes only works for distances larger than 0.5m.

Table 1. PLR and FPR for different distances between the transmitter and receiver

Distance	PLR	FPR	Pulse Voltage	Size of dataset
0.5m	$< 2.16 \cdot 10^{-6}$	$4.0 \cdot 10^{-6}$	3.0V	925,936 cycles
0.75m	$< 1.05 \cdot 10^{-5}$	$3.37 \cdot 10^{-4}$	3.0V	189,880 cycles
1.0m	$3.32 \cdot 10^{-7}$	$1 \cdot 10^{-6}$	3.0V	6,026,342 cycles
3.8m	$< 1.62 \cdot 10^{-6}$	$9.4 \cdot 10^{-5}$	6.0V	617,190 cycles

In table 1, one can see that the dataset for a distance of one meter is the largest. This is intentional and based on the fact that the desired cell size is one meter. The distance of 3.8m represents the maximum distance on the the given 2024 aluminum plate described earlier. This number represents the maximum possible distance on that structure. Besides the reliability of the link, the last entry also indicates that the sink, if transmitting at 6V, is capable of reaching any given point on the plate for synchronization purposes. The rather large differences in the FPR are because of the coupling mechanism of the PWAS for that experiment. In our system, the PWAS have not been attached to the structure with an adhesive bonding. The FPR as well as the PLR show promising results considering the fact that the current hardware does not have a bandpass filter.

4.2 Distance estimation

Based on the tested distances from the previous subsection, the performance of the distance estimation is going to be evaluated. Figure 8 shows the results of the distance estimation for a distance of 0.5m, 0.75 and 1.0m. When the distance between the transmitter and receiver was 0.5m, the distance has been estimated by the algorithm described in section 2.2 for 462,967 times. In this experiment, the distance has been estimated to be $d = \bar{d} \pm \sigma = 0.5002m \pm 0.0015m$. This result shows rather high accuracy as well as a low variation in the determination of the distance.

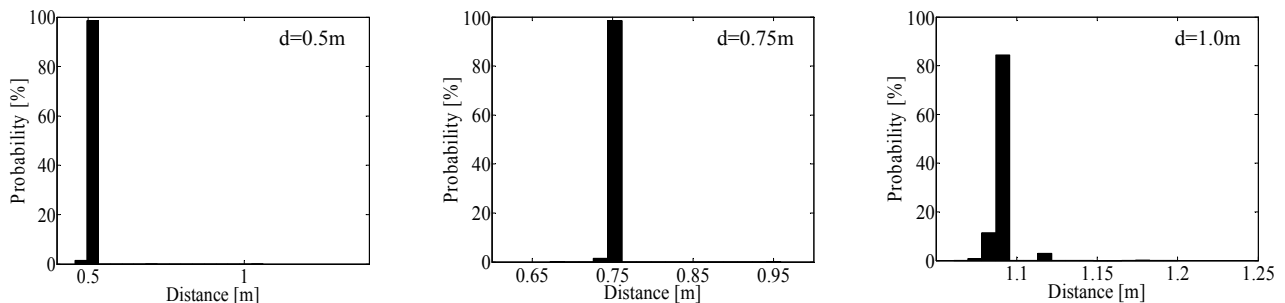


Figure 8. Probability Density Function for estimated distances

Next, the results for the distance estimation for a given distance of 0.75m are being evaluated. The dataset of this estimation holds 94,940 pulses. Based on the information of that experiment, the node estimated the distance to be $0.7495m \pm 0.002m$. Again, this result is accurate and shows a rather low variation. Due to the fact that the proposed cell size is one meter, the distance estimation has been tested for that distance as well. The dataset for this experiment contains 3,013,171 pulses. In this experiment, the distance has been determined to be equal to $1.09m \pm 0.007m$. This

distance estimation shows a rather consistent estimation but has an offset of 10cm. Considering the previous results and the consistency of this one, the source of error most likely is found in the accuracy of setting up the 1.0m distance on the structure before the experiment started. Therefore, the results of this experiment are satisfying as well.

4.3 Measurements of delay spread

In order to determine the minimum slot size to be used the frame structure; the length of the delay spread has to be determined. For this, various absolute distances and locations of the transmitter/receiver pair have been studied on the structure. Also, the transmitting pulse strength (3V, 6V) has been varied as well. In all scenarios, the delay spread showed an upper bound below 10ms. Therefore, the minimum slot size in the frame structure has to be equal to or greater than 10ms. In order to improve the robustness of the system against timing inaccuracy, the slot size λ has been chose to be 15ms, including a 5ms guard time. Incorporating the distance estimation algorithm from section 2.2, may reduce the value of λ , since the length of the guard interval may be reduced.

5. CONCLUSIONS AND FUTURE WORK

The implementation of a novel communication mechanism between nodes in an event monitoring WSN has been introduced. In order to determine the reliability of the communication link, a throughout study of PLR and FPR has been conducted. The outcomes of those experiments have been satisfying and indicate that pulse switching can be used to exchange binary information in a WSN for event sensing and localization. Additionally, it has been shown that the distance between two nodes on a structure can be determined using the properties of lamb wave propagation in solid substrates. In the current system, the slot size has been chosen large enough so that the propagation delay can be ignored in respect to a fully synchronized network. In future, however, the slot size may be reduced further in order to shrink the frame size. In that case, it will be essential that all nodes in the network are rather perfectly synchronized. Then, the distance estimation algorithm will be a powerful tool to determine the propagation delay between a node and the sink. Based on the reception of the synchronization pulse at the beginning of a frame and the determined distance between the two nodes, an accurate synchronization is possible. In respect to the findings presented in this publication, the next step will be to implement the multi hop network in order to allow a communication over an extended network structure. Another branch for future work is the development of a bandpass filter. This will become an essential part of the system, since every structure will introduce noise to the hardware platform.

REFERENCES

- [1] Q. Huo, B. Dong, S. Biswas, "Cellular Pulse Switching: An Architecture for Event Sensing and Localization in Sensor Networks," ICDCN 2013, pp. 208-224
- [2] H. W. Tomlinson, Jr, J. B. Deaton, Jr, E. Nieters, and F. Ross, "Ultrasound communication system for metal structure and related methods," U.S. Patent 765414802-Feb-2010.
- [3] G. J. Saulnier, H. A. Scarton, A. J. Gavens, D. A. Shoudy, T. L. Murphy, M. Wetzel, S. Bard, S. Roa-Prada, and P. Das, "PIG-4 Through-Wall Communication of Low-Rate Digital Data Using Ultrasound," in Ultrasonics Symposium, 2006. IEEE, 2006, pp. 1385 –1389.
- [4] X. Zhao, H. Gao, G. Zhang, B. Ayhan, F. Yan, C. Kwan, and J. L. Rose, "Active health monitoring of an aircraft wing with embedded piezoelectric sensor/actuator network: I. Defect detection, localization and growth monitoring," *Smart Mater. Struct.*, vol. 16, no. 4, p. 1208, Aug. 2007.
- [5] V. Giurgiutiu, A. Zagrai, and J. Bao, "Damage Identification in Aging Aircraft Structures with Piezoelectric Wafer Active Sensors," *Journal of Intelligent Material Systems and Structures*, vol. 15, no. 9–10, pp. 673–687, Sep. 2004.
- [6] V. Giurgiutiu, "Lamb-wave generation with piezoelectric wafer active sensors for structural health monitoring," *Smart Structures and Materials—proceedings of the SPIE*, 5056 (2003), pp. 111 – 122.
- [7] X. Zhang, S. Yuan, and T. Hao, "Lamb wave propagation modeling for structure health monitoring," *Front. Mech. Eng. China*, vol. 4, no. 3, pp. 326–331, Sep. 2009.
- [8] V. Giurgiutiu, "Structural Health Monitoring: with Piezoelectric Wafer Active Sensors," 1st ed. Academic Press, 2007.